Kanninen, Petri; Borghei, Maryam; Hakanpää, Janina; Kauppinen, Esko I.; Ruiz, Virginia; Kallio, Tanja

Temperature dependent performance and catalyst layer properties of PtRu supported on modified few-walled carbon nanotubes for the alkaline direct ethanol fuel cell

Published in:
Journal of Electroanalytical Chemistry

DOI:
10.1016/j.jelechem.2016.10.019

Published: 01/01/2017

Document Version
Peer-reviewed accepted author manuscript, also known as Final accepted manuscript or Post-print

Temperature dependent performance and catalyst layer properties of PtRu supported on modified few-walled carbon nanotubes for the alkaline direct ethanol fuel cell

Petri Kanninen[1], Maryam Borghei[2,3], Janina Hakanpää[1], Esko I. Kauppinen[2], Virginia Ruiz[2,4], Tanja Kallio[1,*]

[1] Research Group of Electrochemical Energy Conversion and Storage, Department of Chemistry, Aalto University, P.O. Box 16100, 00076 AALTO, Finland.

[2] Nanomaterials Group, Department of Applied Physics, Aalto University, P.O. Box 15100, 00076 AALTO, Finland

[3] Biobased Colloids and Materials, Department of Forest Products Technology, Aalto University, P.O.Box 16300, 00076 AALTO, Finland.

[4] IK4-CIDETEC, Paseo Miramón 196, E-20009 Donostia-San Sebastián, Spain.

*Corresponding author; Tel. +358505637567, tanja.kallio@aalto.fi

Abstract

The performance of PtRu on three differently modified few-walled carbon nanotube (FWCNT) supports for ethanol electro-oxidation is evaluated in alkaline media both with rotating disc electrode (RDE) and direct ethanol fuel cell (DEFC) measurements at various temperatures (0-60 °C). FWCNT are modified with oxidative treatment (O-FWCNT), aniline coating (A-FWCNT) and N-doped carbon layer (N-FWCNT). RDE testing shows that A-FWCNT/PtRu outperforms both O-FWCNT/PtRu and N-FWCNT/PtRu especially at high temperatures giving 1.5 times higher current at 60 °C. The poisoning resistance of N-FWCNT/PtRu is high over the temperature range, while O-FWCNT/PtRu and A-FWCNT/PtRu become increasingly poisoned with increasing temperature. Alkaline DEFC testing at 30 °C and 50 °C indicates similar dependence to temperature as in RDE tests. However, only N-FWCNT/PtRu can sustain currents for longer than 20-30 h during constant voltage measurement. SEM images of the catalyst layers reveal that both O-FWCNT/PtRu and A-FWCNT/PtRu form a dense structure with little pores for reactant and product transport explaining the quick performance loss, while large pores are formed with N-FWCNT/PtRu facilitating the transport. These results underline that the

interactions between the catalyst support and the ionomer in the fuel cell catalyst layer are important in forming a suitable pore structure for efficient mass transfer.

Keywords

Ethanol; few-walled carbon nanotube; nitrogen; direct ethanol fuel cell; catalyst layer; alkaline electrolyte

1. Introduction

Direct ethanol fuel cells (DEFC) are emerging as an excellent alternative for powering small electronic devices. Unlike batteries, the "charging" of the DEFC is a simple insertion of fuel, and ethanol is non-toxic liquid with a high energy density (8.3 Wh kg^{-1} or 6.7 Wh dm^{-3}). However, the electro-oxidation of ethanol is complicated due to the carbon-carbon bond in its structure and complete oxidation to CO_2 is limited. Thus, a great deal effort has been dedicated to find new and more active catalysts for ethanol electro-oxidation [1].

A fuel cell catalyst generally consists of active metal nanoparticles which are supported on carbon [2]. Therefore, there are two components that can be changed to improve the activity and stability of the catalyst. A wide variety of different metals has been tested for ethanol electro-oxidation but commonly these catalysts are based on Pt or Pd with other metals alloyed with them [1]. With the discovery of new carbonaceous species like carbon nanotubes and graphene also the study of different catalyst supports has increased in popularity. The support directly affects the catalytic activity of the metal by changing its electronic structure through the bond between them [3]. This bond also determines how well the nanoparticle is attached to the support, in other words its stability. The size and distribution of the nanoparticles is also affected by the support [4]. Carbon nanotubes are a popular choice for their high conductivity and surface area. We have previously tested few-walled carbon nanotubes (FWCNT) as the support for PtRu in direct methanol fuel cells (DMFC) [4] and showed improved methanol electro-oxidation activity compared to carbon black supported PtRu. FWCNT are small carbon nanotubes consisting of 3-5 walls that combine the robustness of multi-walled carbon nanotubes and the smallness

and structural perfection of single-walled carbon nanotubes [5]. For example, the outer layer of FWCNT can be modified with dopants, while the inner layers retain their excellent conductivity.

Lately, the nitrogen-doped graphitic materials like carbon nanotubes and graphene have been proven to be highly active for oxygen reduction and evolution reaction in alkaline media [6,7] indicating it can easily adsorb water, hydroxide ions and oxygen that can help to provide the oxygen that is required for complete ethanol oxidation [2]. Nitrogen-doped supports have also been shown to improve the catalyst nanoparticle distribution on the support due to the anchoring effect of the dopant sites [8-10] and thus, to increase ethanol electro-oxidation rate with Pt [11] and PtSn [12] on carbon nanotubes, Pd on carbon nanospheres [13] and PtSn on carbon [14]. However, these experiments have been made in room temperature and no actual DEFC testing is made as is often case when new catalyst are suggested for application in fuel cells. As fuel cells generally operate between 0 and 100°C, it is important to study the catalysts also at elevated temperatures. On the other hand, without DEFC testing there are limited ways to estimate the effect of the new catalyst to the catalyst layer, which is very important for fuel cell mass transfer and performance. We have shown before that new catalyst supports can have dramatic effects to the general and optimum structure of the catalyst layer in the case of nanofiber supported PtRu [15] and N-doped FWCNTs for DMFCs [16].

In this paper, we have prepared oxygen and nitrogen-modified FWCNT supports with PtRu deposited on them and tested them for ethanol electro-oxidation activity in a rotating disc electrode (RDE) electrochemical cell and in alkaline DEFC at various temperatures.

2. Experimental

2.1 Catalyst material preparation

Few-walled carbon nanotubes (FWCNT) were used as catalyst substrate. In order to study the influence of surface chemistry on the particle size distribution and electrocatalytic activity, FWCNT were modified before nanoparticle deposition. Firstly, FWCNT were functionalized with 2 M HNO_3/1 M H_2SO_4 (1:1) at 120 °C for 4 h to introduce oxygen functional groups on the surface (O-FWCNT). Secondly, FWCNT were treated with aniline (A-FWCNT) to introduce positive charge on the surface [17]. Aniline (20 wt% ratio) was mixed with isopropanol/water (1:1) and then FWCNT added to the solution in the sonication

bath for 3 h at 45 °C. Finally, N-doped FWCNT (N-FWCNT) were synthesized according to the procedure described previously [18]. Briefly, FWCNT were coated with polyaniline via chemical polymerization of aniline with ammonium persulfate (APS) in 1 M HCl, followed by pyrolysis at 900 °C for 1 h. This forms an N-doped layer of carbon on the FWCNT.

PtRu nanoparticles (25 wt%, Pt:Ru 1:1 atomic ratio) were deposited on the substrates via a polyol method by reduction of K_2PtCl_6 and $RuCl_3$ with $NaBH_4$ as reported elsewhere [19]. All chemicals pertaining to the synthesis were acquired from Sigma-Aldrich.

2.2 Rotating disc electrode preparation

Catalyst ink was prepared by mixing the synthesized catalysts of 25 wt% PtRu on O-FWCNT, N-FWCNT and A-FWCNT with N-methyl-2-pyrrolidone (NMP, Sigma-Aldrich) and 12 wt % solution of FAA3 ionomer in NMP (Fumatech). A catalyst ink contained 5 mg of catalyst, 6 µl of FAA3 solution and 200 µl of NMP. The components were first mixed by a magnetic stirrer for 30 min, then subjected to 15 min of sonication and finally mixed by a magnetic stirrer for 4 h. Four glassy carbon electrodes (GCE, diameter 5 mm, Pine Instruments) were polished and a 5 µl aliquot of the ink was dropped on each of the GCEs. The electrodes were then put in vacuum oven and kept at 60°C for 1 h to evaporate the NMP. All electrodes were measured within 4 days from their preparation.

2.3 Rotating disc electrode measurements

A 3-electrode electrochemical cell with a rotating working electrode (Pine) was assembled with a modified GCE as the working electrode, Pt-wire as the counter electrode and mercury/mercury oxide (0.1 M NaOH) reference electrode. All potential values were converted to the reversible hydrogen electrode (RHE) scale. The electrolyte was 0.1 M NaOH (Merck). A Metrohm Autolab PGSTAT100 potentiostat was used to control the potential of the cell. First, the cell was de-aerated by bubbling with N_2 for 30 minutes. A cyclic voltammogram was made to determine that the electrode preparation had been successful. The catalyst surface was cleaned and its active area was determined with CO adsorption. The electrolyte was bubbled with CO (99.99%, Aga) for 30 min with the GCE rotating at 300 rpm to enhance the mass transfer to the electrode. Then the cell was purged from non-adsorbed CO with N_2

(99.999%, Aga). The cell potential was held at 0.125 V vs RHE during this time. Subsequently, 3 cyclic voltammograms were measured at 10 mV s^{-1}. CO oxidation charge was determined by subtracting the second scan from the first and calculating the area under the CO oxidation peak between the potential where subtracted current becomes positive and 0.82 V vs RHE. The charge was converted to area by using the value 420 mC cm^{-2} for the oxidation of an adsorbed monolayer of CO on a PtRu surface [20]. It is worth noting that this figure is an approximation derived for a pure Pt surface as the exact nature of CO absorption on a Ru surface is yet unknown and thus, it should only be used to calculate the surface area for the comparison of catalysts with similar structures. All the currents pertaining to RDE measurements are normalized with the active area derived from the CO oxidation. The electrode was further cleaned with 5 cyclic voltammograms between 0.075 and 0.825 V vs RHE. The potential was not raised higher due to Ru dissolution [21]. These measurements were made at room temperature.

Next, the electrolyte was changed to 0.1 M NaOH and 1 M ethanol (Altia Industrial) solution and the cell was heated or cooled to the studied temperature (0, 20, 40 and 60°C) while bubbling with N_2 and potential being held at 0.075 V vs RHE. Modified GCEs made from the same ink were used to measure the different temperatures to minimize the effect of ink constitution variation. However, each temperature was measured with different GCE to minimize the degradation of the catalyst during measurements. Care was taken to make sure that the cell was as tightly closed as possible so that ethanol would not evaporate significantly during measurements. The inlet gas was also directed through a gas bubbler with the same solution as in the cell. Cyclic voltammograms (CV) were then recorded with 1800 rpm rotation. Catalyst poisoning was studied with a 2000 s and repeated 300 s chronoamperometric measurements at 0.5 V vs RHE with 1800 rpm rotation.

2.4 MEA preparation

A FAA3 membrane (Fumatech) was ion-exchanged in 0.5 M NaOH (Merck) with stirring for 1 h and washed in deionized water. Before assembling the fuel cell, the membrane was soaked in 1 M ethanol. The catalyst ink was prepared by mixing the synthesized catalysts (O-FWCNT/PtRu, A-FWCNT/PtRu and N-FWCNT/PtRu) with NMP, isopropanol (Merck) and 12 wt % solution of FAA3 ionomer in NMP. The components were first mixed by a magnetic stirrer for 30 min, then subjected to 15 min of sonication and finally mixed by a magnetic stirrer overnight. Isopropanol was added to the ink during mixing until

the viscosity of the ink was suitable for air brush painting. The resulting slurry was painted on a pre-weighted gas diffusion layer (GDL) with a microporous layer (FuelCellEtc GDL-CT) by an air brush and dried in a vacuum oven at 40 °C for 1.5 h. The GDL was then weighed to determine the weight of the dry catalyst layer. The PtRu loadings for each successfully fabricated anode were as follows (in mg cm^{-2}): 0.61 (FWCNT), 0.94 (N-FWCNT) and 0.81 (A-FWCNT). Due to the variance of the catalyst loadings, the fuel cell anode polarization currents in this study are normalized in respect to PtRu mass. A commercial carbon cloth electrode with 4 mg cm^{-2} of Pt black (FuelCellEtc HLGDE) was used as the cathode after it was sprayed with FAA3 ionomer (0.35 mg cm^{-2} ionomer loading). The MEA was not hot-pressed due to the sensitivity of the FAA3 membrane towards pressure and temperature [22].

The catalyst layers for conductivity measurements were prepared similarly as the ones for fuel cell measurement but sprayed on a plastic film. Conductivity was measured in-plane by a linear potential sweep with a 4-electrode probe (Bekktech) and calculated from the slope of the voltage-current plot. These samples were also used for scanning electron microscopy (SEM, JEOL JSM-7500FA) to study the structure of the catalyst layer.

2.5 Fuel cell experiments

The fuel cell was assembled with Teflon® gaskets, carbon cloth gas diffusion layers and a MEA. The cell was then clamped together with eight screws and tightened to a torque of 5 Nm. The active area of the fuel cell was 5.29 cm^2. Cell voltage and current were controlled by a Metrohm Autolab PGSTAT20 potentiostat with a BSTR10A booster. Prior to the measurement, the cell was first allowed to stabilize overnight at 50°C, with a 0.2 ml min^{-1} flow of 1 M ethanol solution in deionized water at the anode and 100 ml min^{-1} flow dry O_2 (99.999%, Aga) at the cathode, while constant current of 0.5 mA cm^{-2} was applied.

The next day O_2 at the cathode was replaced with H_2 (99.999%, Aga) after N_2 (99.999%, Aga) flushing and the flow rates increased to 2.0 ml min^{-1} for ethanol and 200 ml min^{-1} for H_2. Once stabilized, anode polarization curves were measured with a voltage sweep from the open circuit voltage (OCV, ~0.01 V) to 0.5 V at a rate of 2 mV s^{-1} followed by cooling of the fuel cell to 30°C and measurement of another set of anode polarization curves. Subsequently, the H_2 at the cathode was changed to O_2 and the flow rates reduced to 0.3 ml min^{-1} and 100 ml min^{-1}, for the ethanol and O_2 respectively, while the cell was

heated back to 50 °C. The cell was stabilized at OCV for 30 minutes prior to a 2-day (44 h) galvanostatic (1.5 mA cm^{-2}) measurement. After 44 h or when cell voltage was 0 V, the measurement was stopped for 2 minutes and new galvanostatic measurement was started to observe the differences in catalyst activity. The total time under constant current was approximately 50 h for each catalyst.

3. Results and discussion

3.1 Catalyst properties

TEM images of the synthesized catalysts with PtRu particle size distribution are presented in Fig. 1. The average particle size and the elemental composition of PtRu are presented in Table 1. It can be observed that PtRu nanoparticles are more evenly distributed on N-FWCNT and especially clustered on O-FWCNT. This is in line with previous observations [23-25] indicating that N-moieties create targets for metal deposition on carbon supports. On the other hand, PtRu nanoparticles formed on A-FWCNT show some clustering, which points to the fact that just having nitrogen-containing substances on FWCNT does not improve nanoparticle distribution as much as having nitrogen doped into the graphitic carbon. The average size of the nanoparticles supports this observations as it decreases in the sequence of O-FWCNT/PtRu > A-FWCNT/PtRu > N-FWCNT/PtRu (Table 1).

The total metal content of N-FWCNT/PtRu is significantly higher than of the other two catalysts (Table 1). This is expected as nitrogen is more electronegative than carbon and causes negative charge on the nitrogen atom and positive charges on the adjacent carbon atoms. These charges attract the metal precursor ions to form nanoparticles. For O- and A-FWCNT, the charged groups are single charged pending groups that may be less effective in anchoring metal precursors as their charge is dependent on their protonation degree. Properties of the modified FWCNT also affect the ratio of the metals: N-FWCNT/PtRu is close to the intended 50:50 atomic ratio between Pt and Ru, while A-FWCNT/PtRu and O-FWCNT/PtRu have higher Pt content (Table 1).

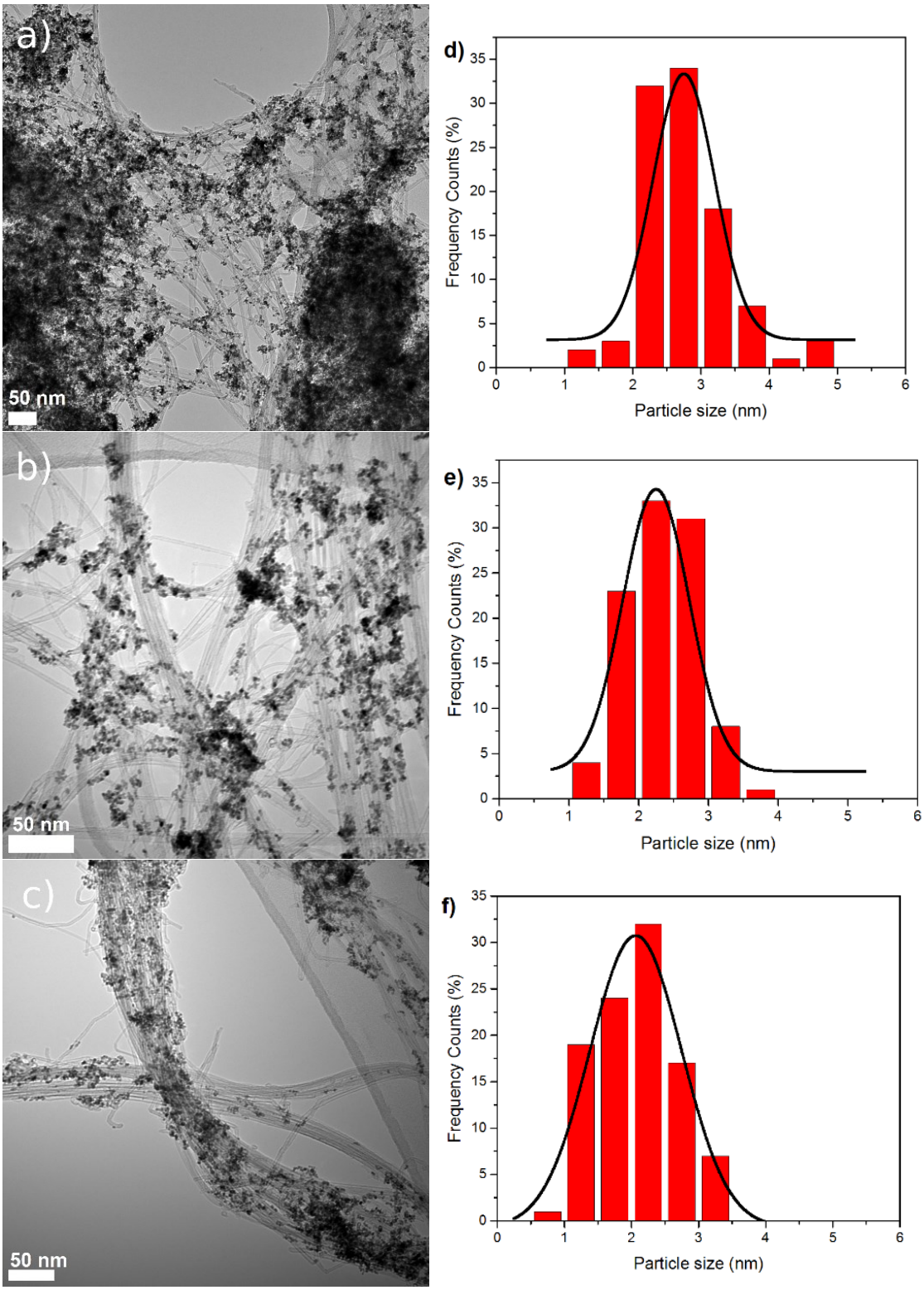

Figure 1. TEM images of the synthesized catalysts (a-c) and their PtRu nanoparticle size distributions (d-f). a,d) O-FWCNT/PtRu, b,e) A-FWCNT/PtRu and c,f) N-FWCNT/PtRu.

Table 1. Physical properties of the synthesized catalysts.

Sample	O-FWCNT/PtRu	A-FWCNT/PtRu	N-FWCNT/PtRu
Max Gauss peak (nm)	2.75	2.25	2.06
Average size (nm)	2.73	2.34	2.08
Metal wt% (EDX)	24.1	23.8	28.8
Pt (wt%)	18.3	19.4	20.2
Ru (wt%)	5.8	4.4	8.6
Pt:Ru (at%)	62:38	70:30	55:45

3.2 RDE measurements

RDE electrodes were first characterized in pure electrolyte (0.1 M NaOH). The CVs for the different catalysts (Fig. 2a) shows different peak potentials for the hydrogen desorption between 0.075 and 0.35 V. It can be seen that A-FWCNTs/PtRu with the least Ru content demonstrated the peak at a lower potential than the others. Similar effect has also been observed with decreasing Ru content elsewhere [25] explaining the difference. It is also possible that the interactions of the modified supports and the PtRu nanoparticles play a role in the shape of the peak [25].

The electrochemically active surface area (EASA) was determined from the CO oxidation (Figure 2b) and following values were determined: O-FWCNT/PtRu 99±7 m^2/g, A-FWCNT/PtRu 59±2 m^2/g and N-FWCNT 101±1 m^2/g. The values represent the average from 4 electrodes used in the determination of the ethanol electro-oxidation activity. The EASA of O-FWCNT/PtRu and N-FWCNT/PtRu are approximately 100 $m^2\ g^{-1}$, which is high for carbon supported catalysts but not unusual for CNT supported PtRu catalysts [25-27]. For the A-FWCNT/PtRu, the active area is only about half of the other catalysts which can be due to aniline covering some pores of the FWCNT. The CO oxidation starts at 20 to 30 mV lower potentials with the N-modified catalyst than with unmodified catalyst indicating the known beneficial effect of N species in the catalyst supports to CO tolerance [28]. The negative shift and sharpening of the peak with A-FWCNT/PtRu may again be due to the low Ru content as has been shown in acidic conditions [29].

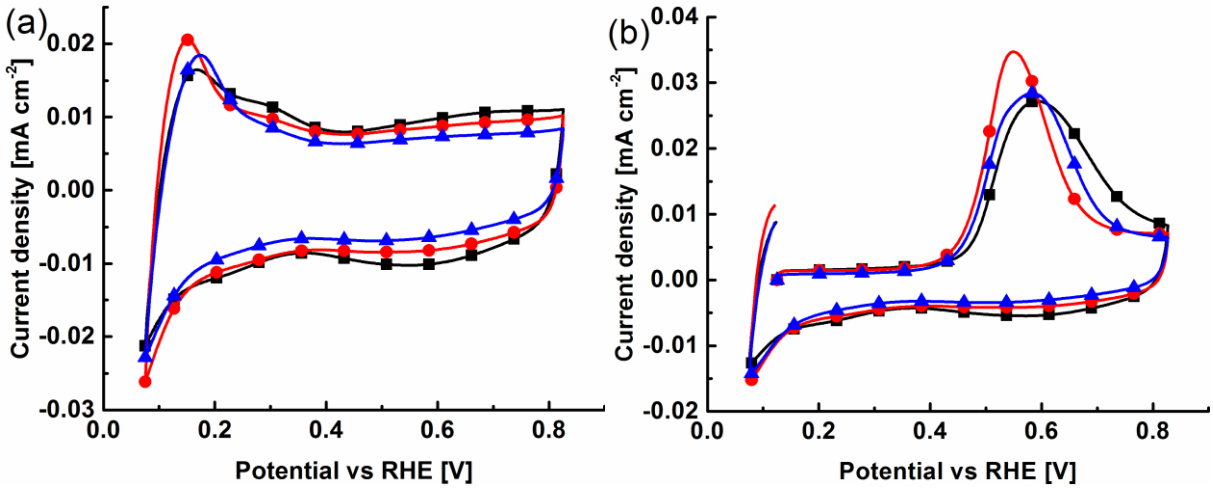

Figure 2. a) The CVs and b) adsorbed CO layer oxidation of the different catalyst in 0.1 M NaOH, room temperature and stationary electrode. ■ O-FWCNT/PtRu, ● A-FWCNT/PtRu, ▲N-FWCNT/PtRu.

The cyclic voltammograms in 0.1 M NaOH containing 1 M ethanol were performed at 1800 rpm after the CO oxidation (Fig. 3). All the catalysts were measured in 0, 20, 40 and 60°C. In all the temperatures, A-FWCNT/ PtRu exhibited superior performance, while N-FWCNT/PtRu had the lowest performance except at 60°C, where it had similar activity compared with O-FWCNT/PtRu. The low performance of the N-FWCNT/PtRu is surprising as nitrogen-doping of the carbon support commonly improves the ethanol oxidation activity of metals [11,12]. However, N-doping does not always have significant effect on the methanol oxidation activity of supported PtRu [30] and some N-doped carbon materials perform worse than undoped Vulcan supports [31,32]. Therefore, the same can apply to ethanol oxidation. Also, the small amount of nitrogen (~0.5 at% [18]) in the structure can explain the poor performance of N-FWCNT/PtRu [33,34]. Finally, the Pt:Ru ratios of the catalysts differ significantly, which affects the ethanol electro-oxidation activity. Bagchi et al. [35] determined Pt:Ru ratio 60:40 to be optimum for Ni supported PtRu in alkaline media, which is close to the ratios of both O-FWCNT/PtRu (62:38) and N-FWCNT/PtRu (55:45). This does not explain the excellent performance of A-FWCNT/PtRu as its Pt:Ru ratio is higher 70:30. However, in acidic media several optimum values for Ru content for ethanol electro-oxidation have been determined in the range from 18 to 50 at% [36-39], so it is likely that the optimum content in alkaline is also highly sensitive to synthesis method, measurement conditions [40], and alloying degree of Ru [41]. However, the current values in a potential relevant to DEFC (0.5 V) show

that A-FWCNT/PtRu is clearly the most effective only at 60 °C (Fig. 4). The performances of the catalysts do not differ significantly until at high temperatures justifying their further testing. All the catalyst passivate during the CV meaning that the current at 0.5 V on the positive sweep is lower than on the negative sweep due to poisoning at low potentials by reaction intermediates as well as the cleaning of the surface by oxidation at high potentials [42].

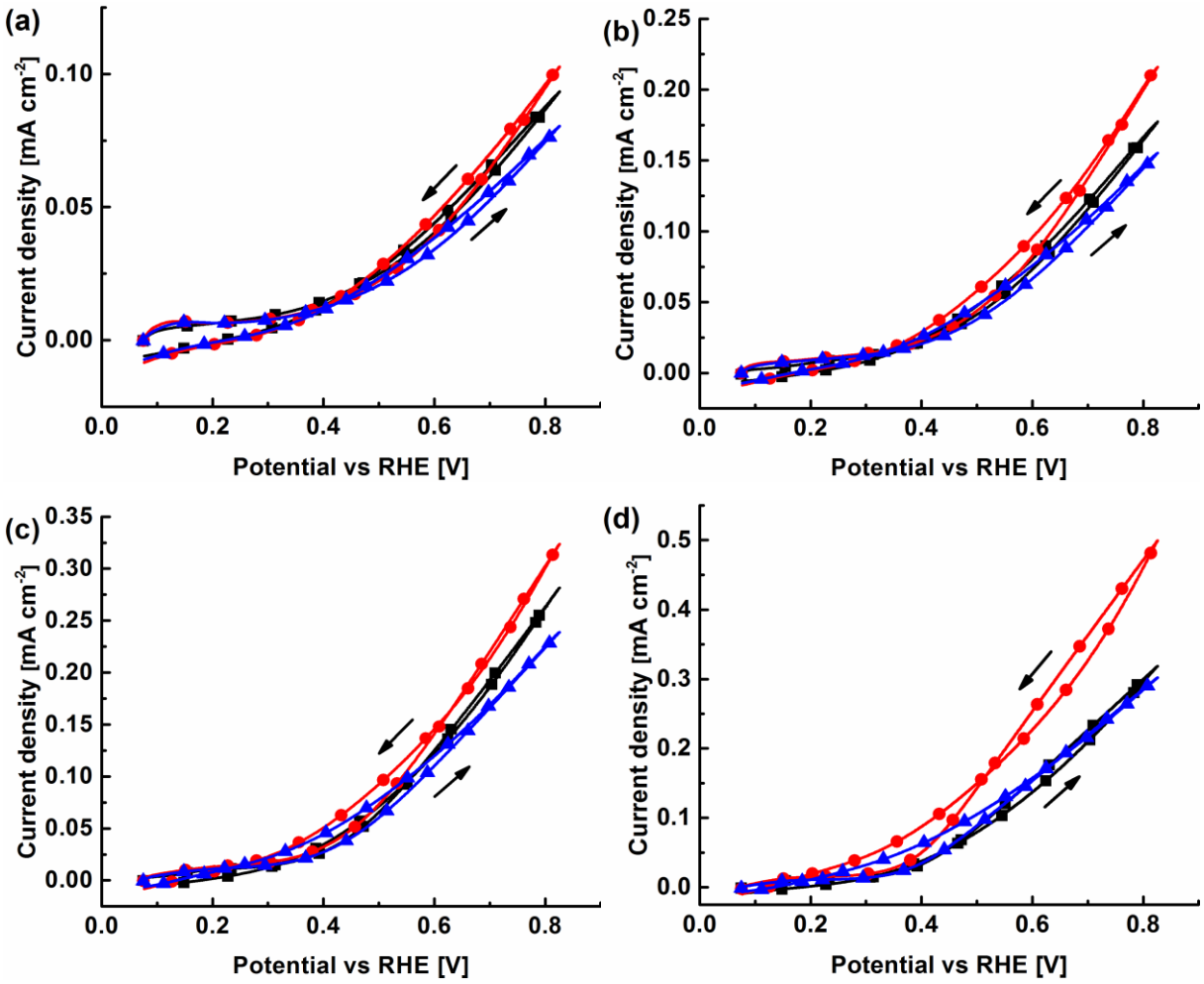

Figure 3. Ethanol electro-oxidation currents in 0.1 M NaOH containing 1 M ethanol with 1800 rpm at various temperatures: a) 0 °C, b) 20 °C, c) 40 °C and d) 60 °C. ■ O-FWCNT/PtRu, ● A-FWCNT/PtRu, ▲N-FWCNT/PtRu.

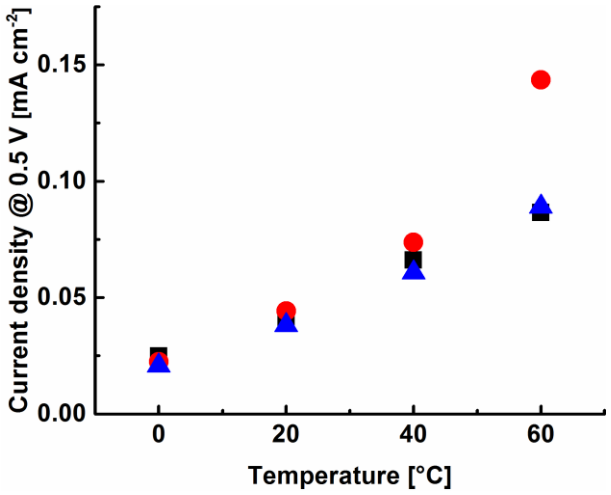

Figure 4. Ethanol electro-oxidation currents sampled at 0.5 V vs RHE (positive sweep) in 0.1 M NaOH containing 1 M ethanol with 1800 rpm rotation and at various temperatures. a) 0 °C, b) 20 °C, c) 40 °C and d) 60 °C. ■ O-FWCNT/PtRu, ● A-FWCNT/PtRu, ▲N-FWCNT/PtRu.

Apparent activation energy ($E_{a,app}$) for ethanol electro-oxidation at different potentials was calculated from the negative sweep of a stationary CV (Fig. 5) [43]. It indicates that N-modification has a clear impact on the reaction as the potential dependence is different for O-FWCNT/PtRu compared to the other catalysts. The $E_{a,app}$ of O-FWCNT/PtRu is between 10 and 15 kJ mol^{-1} and shows a maximum at 0.45 V, while both N-modified catalysts follow a decreasing $E_{a,app}$ tendency over the potential range from 0.3 to 0.8 V. The energies decrease from 25 to 7 kJ mol^{-1} for N-FWCNT/PtRu and from 30 to 12 kJ mol^{-1} for A-FWCNT/PtRu. $E_{a,app}$ for ethanol-oxidation with undoped carbon supports and Pt in alkaline conditions has generally been determined between 10 and 25 kJ mol^{-1} on Pt [44-49] and a decrease has been reported with the addition of Ru in acidic media [38]. Thus, the values we have determined are in line with the previous findings. The fact that the activation energy is larger at low potentials and its potential dependence is different for N-modified supports indicates that there is a strong interaction between the support and the catalyst particle. At high potentials the difference between the catalysts is not significant. The change in the activation energy over potential suggests that there is a change in the reaction mechanism for A- and N-FWCNT/PtRu. It has been shown that at low potentials ethanol dissociates to CO and CH_x on Pt and at high potential ethanol oxidizes to acetaldehyde and further to acetic acid [42]. In the case of O-FWCNT/PtRu, the activation energy is quite stable over the potential range and could mean that the reaction proceeds through one mechanism at all potentials. This could be the oxidation to

acetaldehyde and acetic acid due to the similarity of the $E_{a,app}$ values between the catalysts at high potentials (<0.45 V).

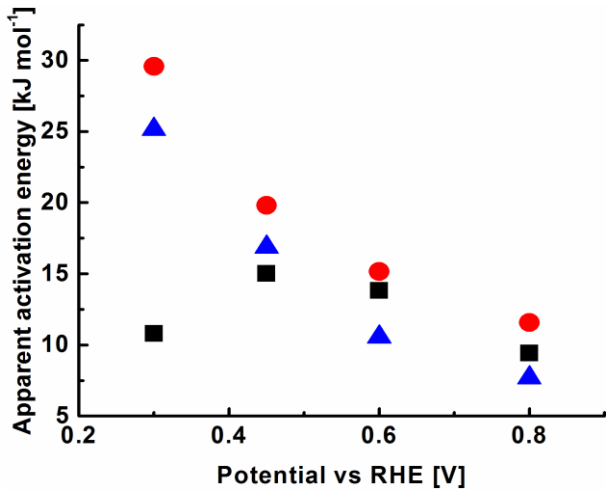

Figure 5. Apparent ethanol electro-oxidation activation energies calculated from CV data at different potentials in in 0.1 M NaOH containing 1 M ethanol. The electrode was stationary and the currents are sampled from the negative scan [43]. ■ O-FWCNT/PtRu, ● A-FWCNT/PtRu, ▲N-FWCNT/PtRu.

The chronoamperometric measurements at 0.5 V at all the temperatures for 2000 s are presented in Fig. 6. O-FWCNT/PtRu shows the highest current at 0 °C as was the case with the CVs at 0.5 V (Fig. 4). The decrease in current is similar for each catalyst indicating a similar tendency for poisoning. However as the temperature rises, the activities of N- and A-FWCNT/PtRu increase more rapidly as expected on the basis of the CV measurements (Fig. 4). N-FWCNT/PtRu is also clearly the most resistant to poisoning at temperatures over 20 °C and retains superior current at the end of the experiment. A-FWCNT/PtRu shows the best current initially but suffers from a high poisoning rate, while O-FWCNT/PtRu suffers from both low initial current and high poisoning rate. The percentage of current remaining at the end of the chronoamperometric measurement compared to the initial current as a function of temperature is presented in Fig. 7 with linear fitting. Interestingly, the fraction of ethanol oxidation current remaining is nearly constant for N-FWCNT/PtRu as temperature increases and slightly decreases for A-FWCNT, while a steep decrease for O-FWCNT/PtRu is observed. This could be due to a different reaction mechanism indicated by the $E_{a,app}$ measurements. Repeating the chronoamperometric measurements (3 times 300 s at 0.5 V with 60 s of "rest period" at 0.075 V in between, not shown) did not reveal any

significant differences in the currents indicating that the poisoning effects can be effectively mitigated by lowering the electrode potential possibly due to species desorption and mixing of the concentration gradients near the electrode closer to bulk concentration.

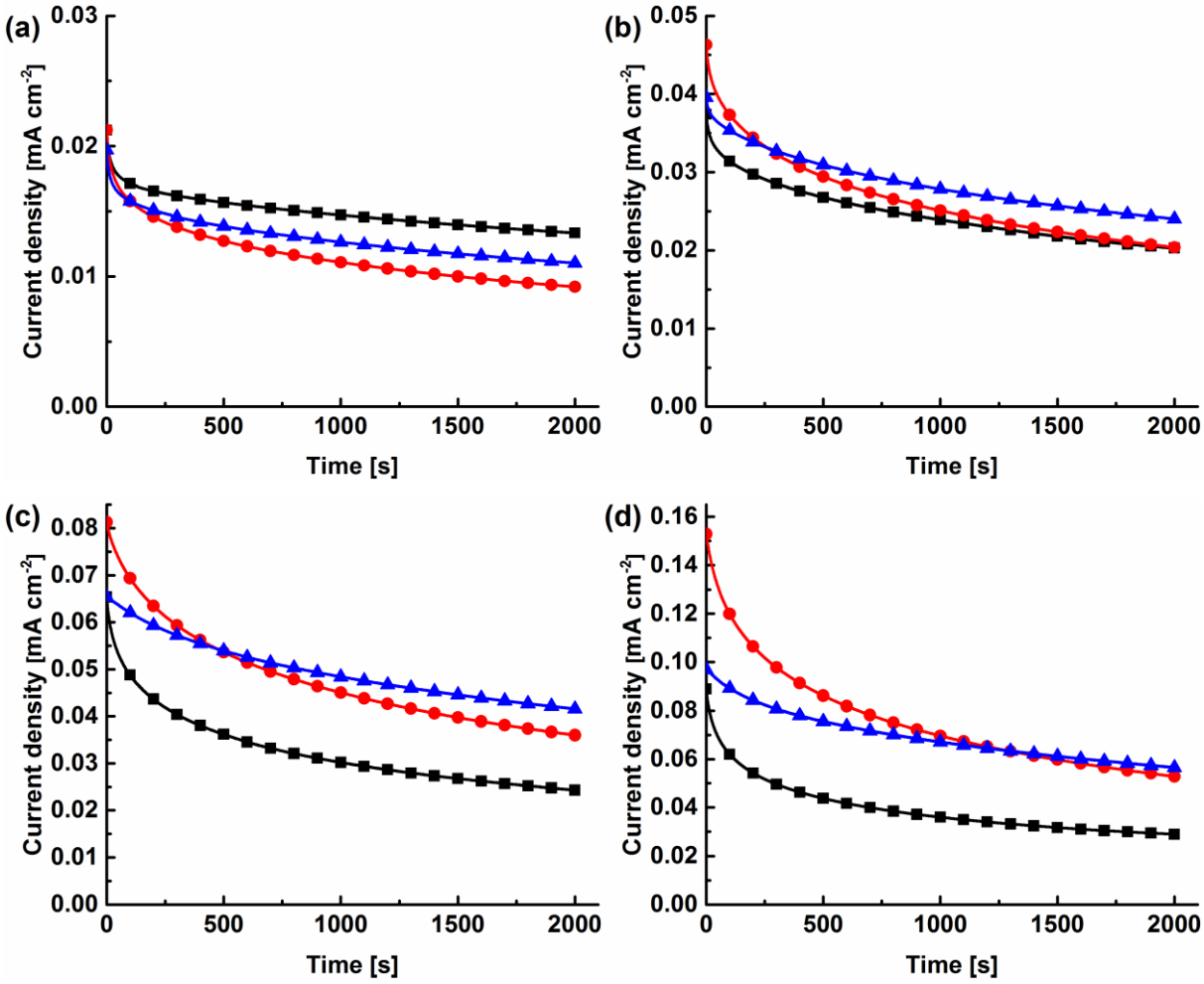

Figure 6. Chronoamperometric measurements (0.5 V vs RHE) for ethanol electro-oxidation in 0.1 M NaOH containing 1 M ethanol with 1800 rpm rotation and at various temperatures for 2000 s: a) 0 °C, b) 20 °C, c) 40 °C and d) 60 °C. ■ O-FWCNT/PtRu, ● A-FWCNT/PtRu, ▲N-FWCNT/PtRu.

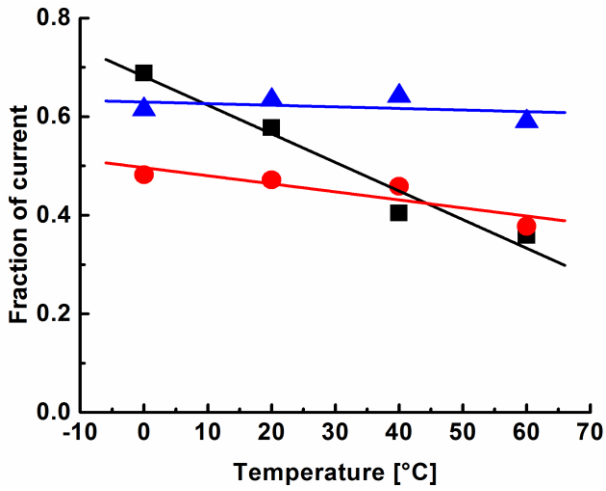

Figure 7. The fraction of ethanol electro-oxidation current remaining at the end of 2000 s chronoamperometric in 0.1 M NaOH containing 1 M ethanol with 1800 rpm rotation as function of temperature for the different catalysts. The lines are linear fits to the data points. ■ O-FWCNT/PtRu, ● A-FWCNT/PtRu, ▲N-FWCNT/PtRu.

3.3 Fuel cell results

MEAs were prepared with the tested catalyst materials as the anode catalyst and ethanol electro-oxidation in alkaline membrane fuel cell conditions was studied with the dynamic H_2 reference electrode technique [50], in which H_2 is fed to the cathode to reduce its polarization and effect to cell performance to a minimum. The resulting polarization curves for each catalyst are presented in Fig. 8. The performance at 30°C corresponds to the RDE results except for N-FWCNT/PtRu, which shows slightly lower current at higher potentials. This could be due to different solid electrolyte and different pH in DEFC as the alkaline membrane will be at least partly saturated with CO_3^{2-} due to presence of CO_2 [51]. Furthermore, the differences may be also related to mass transport properties of the catalyst layers, which does not play a large role in the very thin RDE electrodes. However, when temperature of the fuel cell is increased from 30°C to 50°C, the performance of the A-FWCNT/PtRu and N-FWCNT/PtRu improve compared with O-FWCNT/PtRu in agreement with RDE measurements. This results in N-FWCNT/PtRu showing the best performance at 50 °C. Fuel cell measurement could not be conducted at higher temperatures since the membrane (Fumatech FAA3) becomes unstable in these conditions.

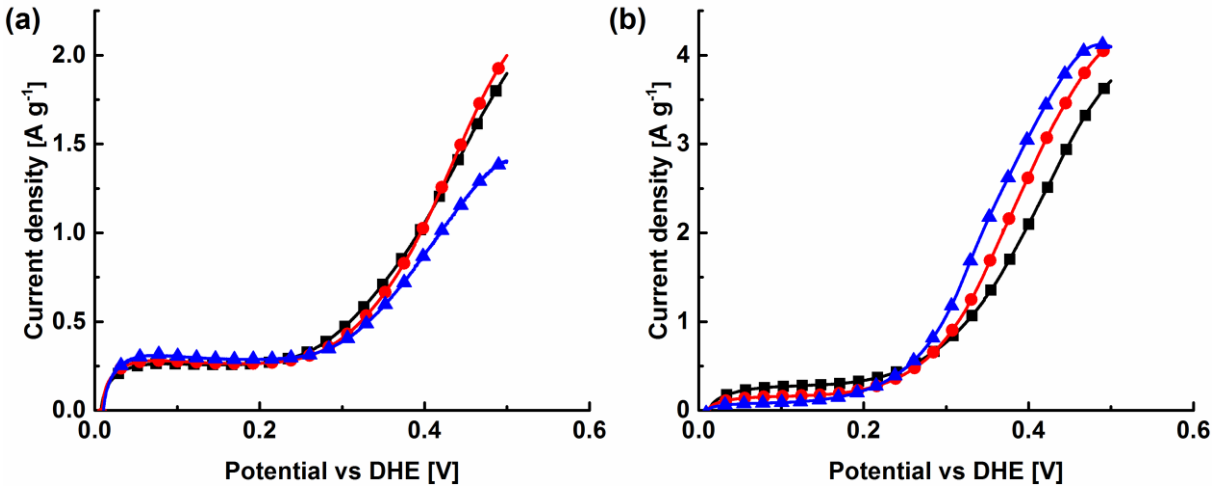

Fig 8. Anode polarization curves in alkaline DEFC with 1 M ethanol at the anode and pure H_2 at the cathode. a) 30 °C, b) 50°C. ■ O-FWCNT/PtRu, ● A-FWCNT/PtRu, ▲N-FWCNT/PtRu.

Chronoamperometric fuel cell measurements at 1.5 mA cm^{-2} and 50°C are presented in Fig. 9a. It is clear that the curves follow the trends observed in the shorter RDE measurements (Fig. 6): N-FWCNT/PtRu is the most stable catalyst, while O-FWCNT/PtRu and A-FWCNT/PtRu lose voltage rapidly until it reaches zero. However, when the chronoamperometric measurement is restarted, N-FWCNT/PtRu follows a slightly lower curve in voltage than before. On the other hand, the performance of O-FWCNT/PtRu remains identical to the first test and the performance of A-FWCNT/PtRu is improved. This is illustrated in Fig. 9b, which shows the potential difference between time points in the two consecutive chronopotentiometric measurements (E_2-E_1). Furthermore, the voltage degradation remains similar in this second measurement: N-FWCNT/PtRu exhibits quite a stable voltage while the voltage of O-FWCNT/PtRu and A-FWCNT/PtRu decrease rapidly. This indicates that despite having good tolerance against poisoning, N-FWCNT/PtRu suffers irreversible changes during fuel cell operation, while the voltage losses observed with O-FWCNT/PtRu and A-FWCNT/PtRu catalysts are reversible and performance is easily recovered by switching the cell off for few minutes (2 minutes at OCV was used in this study). A reason for the irreversible losses for N-FWCNT/PtRu can be the higher potential during the chronopotentiometric measurements: a constant and high cell voltage has been shown to be more detrimental to performance due to cathode degradation in a direct methanol fuel cell [52]. Also, irreversible instability was seen when N-doped FWCNT without metal deposition were tested for the

oxygen reduction reaction (ORR) in alkaline DMFC [16]. Therefore, another reason for instability can be the possible eroding of the thin N-doped carbon layer from the N-FWCNT/PtRu, which would also detach PtRu from the surface. In RDE measurement, the loss of activity was recovered by lowering the electrode potential for all the catalysts. The difference in behavior compared to DEFC conditions in the case of N-FWCNT/PtRu is likely due to the shorter time span of the RDE measurements, which is not long enough to reveal the irreversible losses. The improvement in the performance of A-FWCNT/PtRu between chronoamperometric measurements could be due to aniline dissolving in the ethanol-water fuel solution, which opens new pores in the catalyst layer.

The overall performance of the cells is low compared to previous DEFCs using PtRu as the anode catalyst [53,54] due to the omission of liquid electrolyte (KOH or NaOH) in the fuel solution. However, the use of liquid electrolyte was purposefully avoided in this case as it would cause detrimental carbonate precipitation due to reaction between free cations and carbonate from CO_2 dissolved from ambient air and produced at the anode.

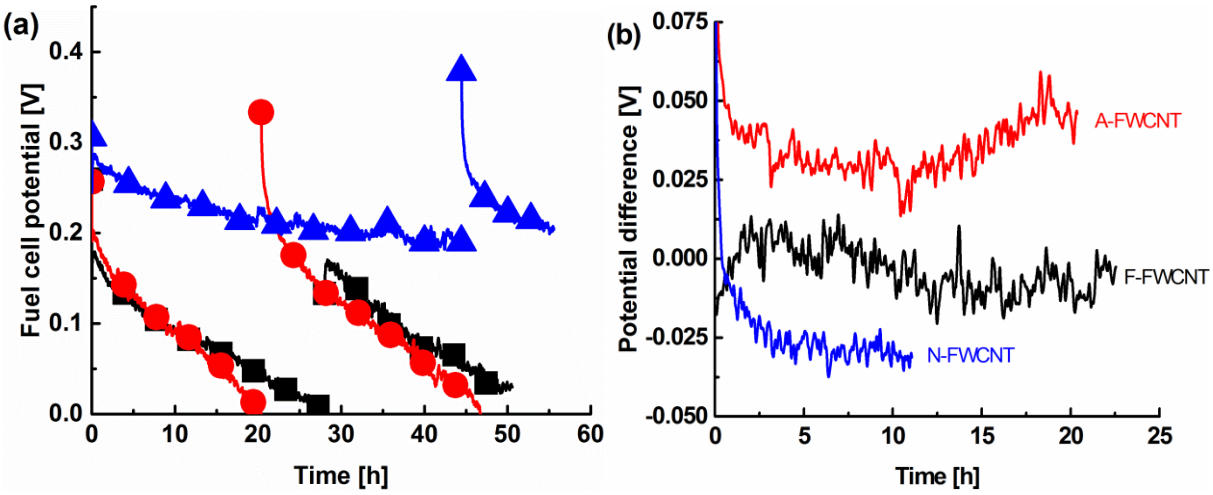

Figure 9. a) Two consecutive chronopotentiometric measurements in DEFC conditions for each catalyst. 1 M ethanol at the anode and pure O_2 at the cathode. The cell was at OCV for 2 min between the measurements. ■ O-FWCNT/PtRu, ● A-FWCNT/PtRu, ▲N-FWCNT/PtRu. b) Difference in voltage between the first and the second measurement (E_2-E_1) as a function of time.

In order to further investigate the reasons for the fuel cell performance, SEM images of the anode catalyst layers are presented in Fig. 10. The total cross-sections of the catalyst layers are presented in Fig. 10a-c with a higher magnification in Fig. 10d-f. Separate catalyst layers were prepared for microscopy analysis as the used MEAs were not feasible for sample preparation. It can be seen that the MEA preparation was successfully carried out to obtain similar thickness of the catalyst layers: average values of 85 μm for O-FWCNT/PtRu, 95 μm for N-FWCNT/PtRu and 88 μm for A-FWCNT/PtRu were determined.

Both A-FWCNT/PtRu and O-FWCNT/PtRu formed a very dense catalyst layer with little pores visible, while N-FWCNT/PtRu has agglomerated structure with large secondary pores between them. Previously, we have observed a similar structure formed by FAA3 and N-FWCNTs without deposited metal catalyst in the cathode catalyst layer [16]. These large secondary pores should facilitate the mass transfer through the whole catalyst layer, while the dense structure of A-FWCNT/PtRu and O-FWCNT/PtRu hinders the transport of ethanol to the active sites and the reaction products from there. This explains the behavior of the MEAs during the chronoamperometric measurement: in the case of O-FWCNT/PtRu and A-FWCNT/PtRu the products accumulate in the catalyst layer decreasing the performance of the fuel cell. However, after stopping the current for a while, the layer is cleaned and performance resumes from higher level resulting in reversible performance loss. With the more open structure in the N-FWCNT/PtRu MEA, reaction products flow out the catalyst layer more easily reducing the reversible performance decrease.

The electrical conductivity of the catalyst layers was also measured with A-FWCNT/PtRu producing the least resistive layer (0.30 Ω cm^2). For O-FWCNT/PtRu and N-FWCNT/PtRu, the resistivity of the layers was higher, 0.96 and 1.00 Ω cm^2, respectively. Although aniline in its monomer form is not electrically conductive, it is possible that some of it has polymerized in the experiments and can be used to enhance the conductivity of a fuel cell catalyst layer. In addition, it is clear that even though N-modification of FWCNT increases the porosity of the catalyst layer, the conductivity of the layer does not suffer from it.

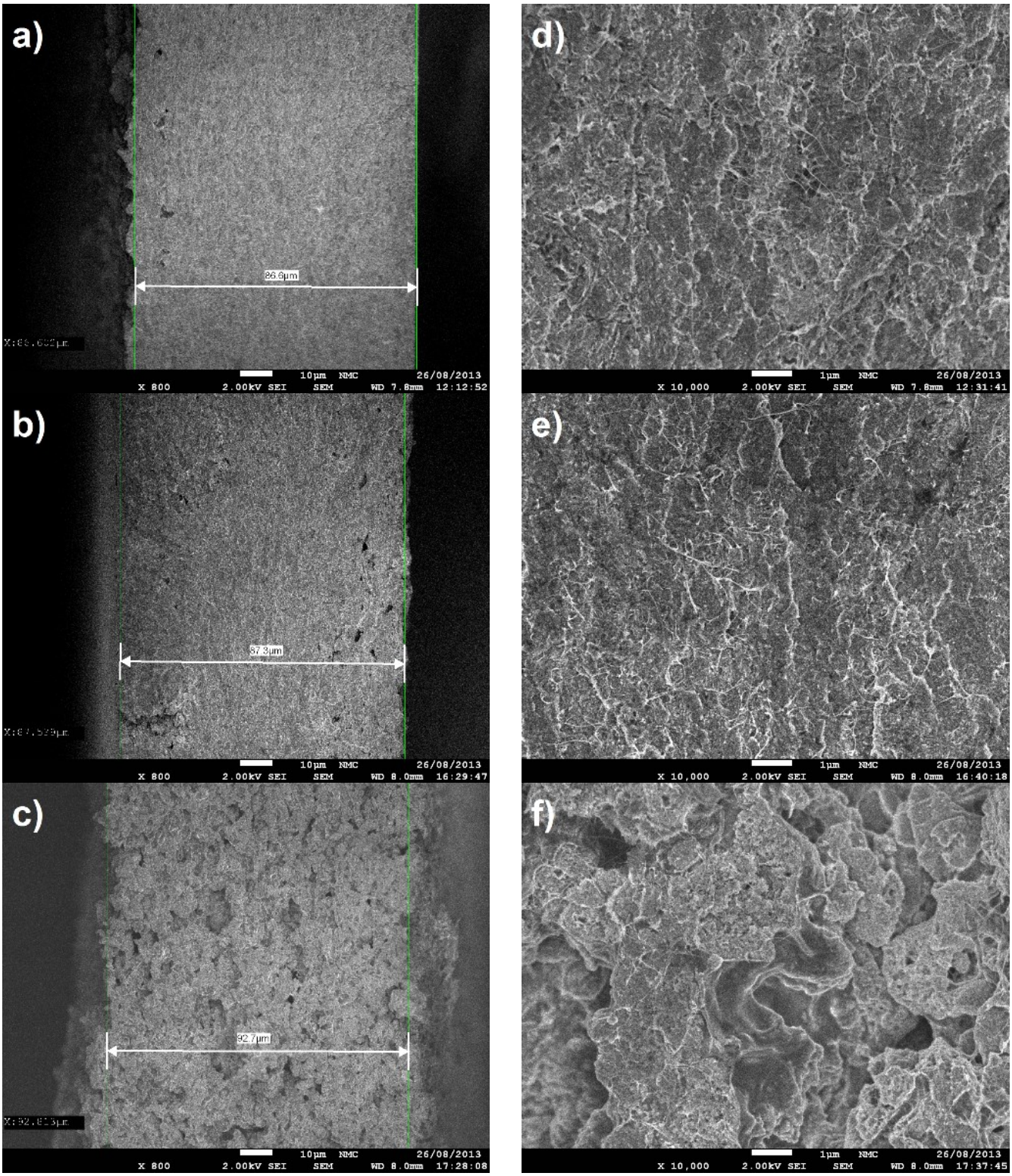

Figure 10. SEM images of the cross-section of the fuel cell anode catalyst layer formed by each catalyst and FAA3 ionomer. a,d) O-FWCNT/PtRu, b,e) A-FWCNT/PtRu and c,f) N-FWNCT/PtRu. a-c) Full catalyst layer cross-section, scale bar 10 µm, d-f) Higher magnification SEM images, scale bar 1µm.

4. Conclusions

In this work, PtRu catalysts supported on differently modified FWCNT have been evaluated for ethanol electro-oxidation in alkaline conditions both in RDE and DEFC configurations at various temperatures. The modification methods were oxidizing the support (O-FWCNT/PtRu), coating it with aniline (A-FWCNT/PtRu) and forming a N-doped layer around carbon nanotube walls (N-FWCNT/PtRu). Both A-FWCNT/PtRu and N-FWCNT/PtRu exhibited improved CO and ethanol electro-oxidation activity especially at higher temperatures (>40 °C) compared to O-FWCNT/PtRu. The activity for ethanol electro-oxidation was highest for A-FWCNT/PtRu while N-FWCNT/PtRu improved poisoning resistance in RDE measurements. The potential dependence of the apparent activation energy for ethanol electro-oxidation on PtRu also changed with the modification of the supports; i.e., it decreased as potential was increased from 0.3 to 0.8 V with A-FWCNT/PtRu and N-FWCNT/PtRu, while O-FWCNT/PtRu had a maximum at 0.45 V. These investigations provide evidence of the beneficial influence of support material modification on the PtRu activity toward ethanol electro-oxidation.

Alkaline DEFC testing of the catalyst showed similar activity and durability as the RDE measurements. However, only N-FWCNT/PtRu could sustain currents for longer than 20-30 h, while during this time the DEFC performance decreased to zero for O-FWCNT/PtRu and A-FWCNT/PtRu. This could be mitigated by a short potential excursion to OCV and restarting the measurement. When the same was done for N-FWCNT/PtRu, small irreversible loss was measured most likely due to the instability of N-doped carbon layer. SEM images of the catalyst layers revealed that both O-FWCNT/PtRu and A-FWCNT/PtRu formed a dense structure with little pores for reactant and product transport with the alkaline ionomer FAA3 explaining the quick and reversible performance loss. On the other hand, large pores were formed with N-FWCNT/PtRu facilitating the transport and improving the performance.

These results underline that the interactions between the catalyst support and the ionomer in the fuel cell catalyst layer are important in forming a suitable pore structure for efficient mass transfer. We have shown previously that N-doping of carbon nanotubes is a promoting factor for forming a porous catalyst layer [16]. Current study confirms this fact for catalyst supports and also reveals that merely adding N-containing species (aniline) to the support is not enough to trigger the formation of a porous structure. Considering the wide variety of carbon supports and their modifications available for fuel cell catalysts, this observation opens a plentiful field for further study and performance improvements.

Acknowledgements

P.K. acknowledges funding from Alfred Kordelin Foundation and from Jane and Aatos Erkko Foundation. T.K. acknowledges funding from Jane and Aatos Erkko Foundation and Academy of Finland. This work made use of the Aalto University Nanomicroscopy Center (Aalto-NMC) premises.

References

[1] A. Brouzgou, A. Podias, P. Tsiakaras, PEMFCs and AEMFCs directly fed with ethanol: a current status comparative review, J. Appl. Electrochem. 43 (2013) 119-136.

[2] E. Antolini, Catalysts for direct ethanol fuel cells, J. Power Sources 170 (2007) 1-12.

[3] J. Nakamura, T. Kondo, Support Effects of Carbon on Pt Catalysts, Top. Catal. 56 (2013) 1560-1568.

[4] M. Borghei, G. Scotti, P. Kanninen, T. Weckman, I.V. Anoshkin, A.G. Nasibulin, S. Franssila, E.I. Kauppinen, T. Kallio, V. Ruiz, Enhanced performance of a silicon microfabricated direct methanol fuel cell with PtRu catalysts supported on few-walled carbon nanotubes, Energy 65 (2014) 612-620.

[5] C. Qian, H. Qi, B. Gao, Y. Cheng, Q. Qiu, L. Qin, O. Zhou, J. Liu, Fabrication of small diameter few-walled carbon nanotubes with enhanced field emission property, J. Nanosci. Nanotechnol. 6 (2006) 1346-1349.

[6] Y. Zhao, R. Nakamura, K. Kamiya, S. Nakanishi, K. Hashimoto, Nitrogen-doped carbon nanomaterials as non-metal electrocatalysts for water oxidation, Nat. Commun. 4 (2013) 2390.

[7] Z. Lin, G.H. Waller, Y. Liu, M. Liu, C. Wong, Simple preparation of nanoporous few-layer nitrogen-doped graphene for use as an efficient electrocatalyst for oxygen reduction and oxygen evolution reactions, Carbon 53 (2013) 130-136.

[8] J. Park, S. Kim, Nitrogen Modified-Reduced Graphene Oxide Supports for Catalysts for Fuel Cells and Their Electrocatalytic Activity, J. Electrochem. Soc. 161 (2014) F518-F524.

[9] M.H. Seo, S.M. Choi, E.J. Lim, I.H. Kwon, J.K. Seo, S.H. Noh, W.B. Kim, B. Han, Toward New Fuel Cell Support Materials: A Theoretical and Experimental Study of Nitrogen-Doped Graphene, ChemSusChem 7 (2014) 2609-2620.

[10] S. Pylypenko, A. Borisevich, K.L. More, A.R. Corpuz, T. Holme, A.A. Dameron, T.S. Olson, H.N. Dinh, T. Gennett, R. O'Hayre, Nitrogen: unraveling the secret to stable carbon-supported Pt-alloy electrocatalysts, Energy Environ. Sci. 6 (2013) 2957-2964.

[11] Z. Zhu, J. Wang, A. Munir, H.S. Zhou, Electrocatalytic activity of Pt nanoparticles on bamboo shaped carbon nanotubes for ethanol oxidation, Electrochim. Acta 55 (2010) 8517-8520.

[12] X. Wang, H. Xue, L. Yang, H. Wang, P. Zang, X. Qin, Y. Wang, Y. Ma, Q. Wu, Z. Hu, Convenient immobilization of Pt–Sn bimetallic catalysts on nitrogen-doped carbon nanotubes for direct alcohol electrocatalytic oxidation, Nanotech. 22 (2011) 395401.

[13] Y. Li, L. Yao, L. Zhang, A. Liu, Y. Zhang, S. Liu, Palladium nanoparticles supported on nitrogen-doped carbon spheres as enhanced catalyst for ethanol electro-oxidation, J. Electroanal. Chem. 730 (2014) 65-68.

[14] H. Wang, Q. Zhao, Q. Ma, PtSn nanoparticles supported on iron nanoparticles wrapped inside nitrogen-doped carbon for ethanol oxidation, Ionics 21 (2015) 1703-1709.

[15] P. Kanninen, M. Borghei, V. Ruiz, E.I. Kauppinen, T. Kallio, The effect of Nafion content in a graphitized carbon nanofiber-based anode for the direct methanol fuel cell, Int. J. Hydrogen Energy 37 (2012) 19082-19091.

[16] P. Kanninen, M. Borghei, O. Sorsa, E. Pohjalainen, E.I. Kauppinen, V. Ruiz, T. Kallio, Highly efficient cathode catalyst layer based on nitrogen-doped carbon nanotubes for the alkaline direct methanol fuel cell, Appl. Catal. , B 156–157 (2014) 341-349.

[17] C. Hsu, H. Liao, P. Kuo, Aniline as a Dispersant and Stabilizer for the Preparation of Pt Nanoparticles Deposited on Carbon Nanotubes, J. Phys. Chem. C 114 (2010) 7933-7939.

[18] M. Borghei, P. Kanninen, M. Lundahl, I. Anoshkin, T. Susi, J. Sainio, A. Nasibulin, T. Kallio, K. Tammeveski, E. Kauppinen, V. Ruiz, High oxygen reduction activity of few-walled carbon nanotubes with low nitrogen content, Appl. Catal. , B 158-159 (2014) 233-241.

[19] A. Santasalo-Aarnio, M. Borghei, I.V. Anoshkin, A.G. Nasibulin, E.I. Kauppinen, V. Ruiz, T. Kallio, Durability of different carbon nanomaterial supports with PtRu catalyst in a direct methanol fuel cell, Int. J. Hydrogen Energy 37 (2012) 3415-3424.

[20] J. Leger, B. Beden, C. Lamy, S. Bilmes, Carbon monoxide electrosorption on low index platinum single crystal electrodes, J. Electroanal. Chem. Interfacial Electrochem. 170 (1984) 305-317.

[21] A.S. Aricò, S. Srinivasan, V. Antonucci, DMFCs: From Fundamental Aspects to Technology Development, Fuel Cells 1 (2001) 133-161.

[22] M. Carmo, G. Doubek, R.C. Sekol, M. Linardi, A.D. Taylor, Development and electrochemical studies of membrane electrode assemblies for polymer electrolyte alkaline fuel cells using FAA membrane and ionomer, J. Power Sources 230 (2013) 169-175.

[23] P.-. Kuo, C.-. Hsu, H.-. Wu, W.-. Hsu, D. Kuo, Controllable-Nitrogen Doped Carbon Layer Surrounding Carbon Nanotubes as Novel Carbon Support for Oxygen Reduction Reaction, Fuel Cells (Weinheim, Ger.) 12 (2012) 649-655.

[24] J. Imran R., N. Rajalakshmi, S. Ramaprabhu, Nitrogen doped graphene nanoplatelets as catalyst support for oxygen reduction reaction in proton exchange membrane fuel cell, J. Mater. Chem. 20 (2010) 7114-7117.

[25] R. Chetty, S. Kundu, W. Xia, M. Bron, W. Schuhmann, V. Chirila, W. Brandl, T. Reinecke, M. Muhler, PtRu nanoparticles supported on nitrogen-doped multiwalled carbon nanotubes as catalyst for methanol electrooxidation, Electrochim. Acta 54 (2009) 4208-4215.

[26] B. Wu, Y. Li, C. Wang, D. Xue, J. Xiao, High aqueous solubility of carboxylated-carbon nanotubes as support for PtRu nanoparticles: Enhanced dispersion and electrocatalytic performance, Int. J. Hydrogen Energy 39 (2014) 7318-7325.

[27] Y. Zhou, G. Yang, H. Pan, C. Zhu, S. Fu, Q. Shi, D. Du, X. Cheng, J. Yang, C.M. Wai, Y. Lin, Ultrasonic-assisted synthesis of carbon nanotube supported bimetallic Pt-Ru nanoparticles for effective methanol oxidation, J. Mater. Chem. A 3 (2015) 8459-8465.

[28] G. Wu, D. Li, C. Dai, D. Wang, N. Li, Well-Dispersed High-Loading Pt Nanoparticles Supported by Shell−Core Nanostructured Carbon for Methanol Electrooxidation, Langmuir 24 (2008) 3566-3575.

[29] J. Jow, S. Yang, H. Chen, M. Wu, T. Ling, T. Wei, Co-electrodeposition of Pt–Ru electrocatalysts in electrolytes with varying compositions by a double-potential pulse method for the oxidation of MeOH and CO, Int. J. Hydrogen Energy 34 (2009) 665-671.

[30] T.S. Olson, A.A. Dameron, K. Wood, S. Pylpenko, K.E. Hurst, S. Christensen, J.B. Bult, D.S. Ginley, R. O'Hayre, H. Dinh, T. Gennett, Enhanced Fuel Cell Catalyst Durability with Nitrogen Modified Carbon Supports, J. Electrochem. Soc. 160 (2013) F389-F394.

[31] A.R. Corpuz, K.N. Wood, S. Pylypenko, A.A. Dameron, P. Joghee, T.S. Olson, G. Bender, H.N. Dinh, T. Gennett, R.M. Richards, R. O'Hayre, Effect of nitrogen post-doping on a commercial platinum–ruthenium/carbon anode catalyst, J. Power Sources 248 (2014) 296-306.

[32] Z. Lei, M. Zhao, L. Dang, L. An, M. Lu, A. Lo, N. Yu, S. Liu, Structural evolution and electrocatalytic application of nitrogen-doped carbon shells synthesized by pyrolysis of near-monodisperse polyaniline nanospheres, J. Mater. Chem. 19 (2009) 5985-5995.

[33] T. Maiyalagan, Synthesis and electro-catalytic activity of methanol oxidation on nitrogen containing carbon nanotubes supported Pt electrodes, Appl. Catal. , B 80 (2008) 286-295.

[34] G. Wu, R. Swaidan, D. Li, N. Li, Enhanced methanol electro-oxidation activity of PtRu catalysts supported on heteroatom-doped carbon, Electrochim. Acta 53 (2008) 7622-7629.

[35] J. Bagchi, S.K. Bhattacharya, The effect of composition of Ni-supported Pt-Ru binary anode catalysts on ethanol oxidation for fuel cells, J. Power Sources 163 (2007) 661-670.

[36] G.A. Camara, R.B. de Lima, T. Iwasita, The influence of PtRu atomic composition on the yields of ethanol oxidation: A study by in situ FTIR spectroscopy, J. Electroanal. Chem. 585 (2005) 128-131.

[37] M. Chatterjee, A. Chatterjee, S. Ghosh, I. Basumallick, Electro-oxidation of ethanol and ethylene glycol on carbon-supported nano-Pt and -PtRu catalyst in acid solution, Electrochim. Acta 54 (2009) 7299-7304.

[38] J. Datta, S. Sen Gupta, S. Singh, S. Mukherjee, M. Mukherjee, Significant Role of Ru-Oxide Present in the Pt-Ru Alloy Catalyst for Ethanol Electro-Oxidation in Acid Medium, Mater. Manuf. Processes 26 (2011) 261-271.

[39] C. Lee, H. Ojima, M. Umeda, Electrooxidation of C1 to C3 alcohols with Pt and Pt–Ru sputter deposited interdigitated array electrodes, Electrochim. Acta 53 (2008) 3029-3035.

[40] H.A. Gasteiger, N. Markovic, P.N. Ross, E.J. Cairns, Temperature-Dependent Methanol Electro-Oxidation on Well-Characterized Pt-Ru Alloys, J. Electrochem. Soc. 141 (1994) 1795-1803.

[41] F.I. Pires, P.G. Corradini, V.A. Paganin, E. Antolini, J. Perez, Effect of the degree of alloying of PtRu/C (1:1) catalysts on ethanol oxidation, Ionics 19 (2013) 1037-1045.

[42] S.C.S. Lai, M.T.M. Koper, Electro-oxidation of ethanol and acetaldehyde on platinum single-crystal electrodes, Faraday Discuss. 140 (2009) 399-416.

[43] J.L. Cohen, D.J. Volpe, H.D. Abruna, Electrochemical determination of activation energies for methanol oxidation on polycrystalline platinum in acidic and alkaline electrolytes, Phys. Chem. Chem. Phys. 9 (2007) 49-77.

[44] A. Dutta, J. Datta, Significant role of surface activation on Pd enriched Pt nano catalysts in promoting the electrode kinetics of ethanol oxidation: Temperature effect, product analysis & theoretical computations, Int. J. Hydrogen Energy 38 (2013) 7789-7800.

[45] S. Sun, Z. Jusys, R.J. Behm, Electrooxidation of ethanol on Pt-based and Pd-based catalysts in alkaline electrolyte under fuel cell relevant reaction and transport conditions, J. Power Sources 231 (2013) 122-133.

[46] A. Santasalo-Aarnio, E. Sairanen, R.M. Arán-Ais, M.C. Figueiredo, J. Hua, J.M. Feliu, J. Lehtonen, R. Karinen, T. Kallio, The activity of ALD-prepared PtCo catalysts for ethanol oxidation in alkaline media, J. Cat. 309 (2014) 38-48.

[47] L.V. Kumar, S. Addo Ntim, O. Sae-Khow, C. Janardhana, V. Lakshminarayanan, S. Mitra, Electro-catalytic activity of multiwall carbon nanotube-metal (Pt or Pd) nanohybrid materials synthesized using microwave-induced reactions and their possible use in fuel cells, Electrochim. Acta 83 (2012) 40-46.

[48] J. Datta, A. Dutta, M. Biswas, Enhancement of functional properties of PtPd nano catalyst in metal-polymer composite matrix: Application in direct ethanol fuel cell, Electrochem. Commun. 20 (2012) 56-59.

[49] S.S. Mahapatra, A. Dutta, J. Datta, Temperature effect on the electrode kinetics of ethanol oxidation on Pd modified Pt electrodes and the estimation of intermediates formed in alkali medium, Electrochim. Acta 55 (2010) 9097-9104.

[50] F. Bresciani, A. Casalegno, M. Zago, R. Marchesi, A Parametric Analysis on DMFC Anode Degradation, Fuel Cells 14 (2014) 386-394.

[51] J.R. Varcoe, P. Atanassov, D.R. Dekel, A.M. Herring, M.A. Hickner, P.A. Kohl, A.R. Kucernak, W.E. Mustain, K. Nijmeijer, K. Scott, T. Xu, L. Zhuang, Anion-exchange membranes in electrochemical energy systems, Energy Environ. Sci. 7 (2014) 3135-3191.

[52] J. Park, J. Lee, J. Sauk, I. Son, The operating mode dependence on electrochemical performance degradation of direct methanol fuel cells, Int. J. Hydrogen Energy 33 (2008) 4833-4843.

[53] A.M. Bartrom, J.L. Haan, The direct formate fuel cell with an alkaline anion exchange membrane, J. Power Sources 214 (2012) 68-74.

[54] A. Verma, S. Basu, Direct alkaline fuel cell for multiple liquid fuels: Anode electrode studies, J. Power Sources 174 (2007) 180-185.